Final COMPASS Results on the Transverse-Spin-Dependent Azimuthal Asymmetries in the Pion-Induced Drell-Yan Process

G. D. Alexeev,[28] M. G. Alexeev,[20,19] C. Alice,[20,19] A. Amoroso,[20,19] V. Andrieux,[33] V. Anosov,[28] K. Augsten,[4] W. Augustyniak,[23] C. D. R. Azevedo,[26] B. Badelek,[25] J. Barth,[8] R. Beck,[8] J. Beckers,[12] Y. Bedfer,[6] J. Bernhard,[30] M. Bodlak,[5] F. Bradamante,[17] A. Bressan,[18,17] W.-C. Chang,[31] C. Chatterjee,[17] M. Chiosso,[20,19] A. G. Chumakov,[29,*] S.-U. Chung,[12,‡‡,§§] A. Cicuttin,[17,16] P. M. M. Correia,[26] M. L. Crespo,[17,16] D. D'Ago,[18,17] S. Dalla Torre,[17] S. S. Dasgupta,[14] S. Dasgupta,[17,‖] F. Delcarro,[20,19] I. Denisenko,[28] O. Yu. Denisov,[19] S. V. Donskov,[29] N. Doshita,[22] Ch. Dreisbach,[12] W. Dünnweber,[13] R. R. Dusaev,[29] D. Ecker,[12] D. Eremeev,[29] P. Faccioli,[27] M. Faessler,[13] M. Finger,[5] M. Finger, Jr.,[5] H. Fischer,[10] K. J. Flöthner,[8] W. Florian,[17,16] J. M. Friedrich,[12] V. Frolov,[28,30] L. G. Garcia Ordòñez,[17,16] F. Gautheron,[7,33] O. P. Gavrichtchouk,[28] S. Gerassimov,[29,12] J. Giarra,[11] D. Giordano,[20,19] A. Grasso,[20,19] A. Gridin,[28] M. Grosse Perdekamp,[33] B. Grube,[12] M. Grüner,[8] A. Guskov,[28] P. Haas,[12] D. von Harrach,[11] R. Heitz,[33] M. Hoffmann,[8] N. d'Hose,[6] C.-Y. Hsieh,[31] S. Huber,[12] S. Ishimoto,[22,††] A. Ivanov,[28] T. Iwata,[22] V. Jary,[4] R. Joosten,[8] E. Kabuß,[11] F. Kaspar,[12] A. Kerbizi,[18,17] B. Ketzer,[8] A. Khatun,[6] G. V. Khaustov,[29] F. Klein,[9] J. H. Koivuniemi,[7,33] V. N. Kolosov,[29] K. Kondo Horikawa,[22] I. Konorov,[29,12] V. F. Konstantinov,[29,†] A. Yu. Korzenev,[28] A. M. Kotzinian,[1,19] O. M. Kouznetsov,[28] A. Koval,[23] Z. Kral,[5] F. Krinner,[12] F. Kunne,[6] K. Kurek,[23] R. P. Kurjata,[24] A. Kveton,[5] K. Lavickova,[4] S. Levorato,[30,17] Y.-S. Lian,[31,¶¶] J. Lichtenstadt,[15] P.-J. Lin,[32] R. Longo,[33,*] V. E. Lyubovitskij,[29,§] A. Maggiora,[19] A. Magnon,[14,†] N. Makke,[17] G. K. Mallot,[30,10] A. Maltsev,[28] A. Martin,[18,17] J. Marzec,[24] J. Matoušek,[5] T. Matsuda,[21] G. Mattson,[33] C. Menezes Pires,[27] F. Metzger,[8] M. Meyer,[33,6] W. Meyer,[7] Yu. V. Mikhailov,[29,†] M. Mikhasenko,[13,‡] E. Mitrofanov,[28] D. Miura,[22] Y. Miyachi,[22] R. Molina,[17,16] A. Moretti,[18,17] A. Nagaytsev,[28] D. Neyret,[6] M. Niemiec,[25] J. Nový,[4] W.-D. Nowak,[11] G. Nukazuka,[22] A. G. Olshevsky,[28] M. Ostrick,[11] D. Panzieri,[19,¶] B. Parsamyan,[1,19,30,*] S. Paul,[12] H. Pekeler,[8] J.-C. Peng,[33] M. Pešek,[5] D. V. Peshekhonov,[28] M. Pešková,[5] S. Platchkov,[6] J. Pochodzalla,[11] V. A. Polyakov,[29] M. Quaresma,[27,*] C. Quintans,[27] G. Reicherz,[7] C. Riedl,[33] D. I. Ryabchikov,[29,12] A. Rychter,[24] A. Rymbekova,[28] V. D. Samoylenko,[29] A. Sandacz,[23] S. Sarkar,[14] T. Savada,[31] I. A. Savin,[28,†] G. Sbrizzai,[17] H. Schmieden,[9] A. Selyunin,[28] K. Sharko,[29] L. Sinha,[14] D. Spülbeck,[8] A. Srnka,[2] M. Stolarski,[27] M. Sulc,[3] H. Suzuki,[22,**] S. Tessaro,[17] F. Tessarotto,[17,*] A. Thiel,[8] F. Tosello,[19] A. Townsend,[33,‖‖,*] T. Triloki,[17] V. Tskhay,[29] B. Valinoti,[17,16] B. M. Veit,[11] J. F. C. A. Veloso,[26] B. Ventura,[6] A. Vijayakumar,[33] M. Virius,[4] M. Wagner,[8] S. Wallner,[12] K. Zaremba,[24] M. Zavertyaev,[29] M. Zemko,[5,4] E. Zemlyanichkina,[28] and M. Ziembicki[24]

(COMPASS Collaboration)

[1]*A.I. Alikhanyan National Science Laboratory, 2 Alikhanyan Br. Street, 0036, Yerevan, Armenia*
[2]*Institute of Scientific Instruments of the CAS, 61264 Brno, Czech Republic*
[3]*Technical University in Liberec, 46117 Liberec, Czech Republic*
[4]*Czech Technical University in Prague, 16636 Prague, Czech Republic*
[5]*Charles University, Faculty of Mathematics and Physics, 12116 Prague, Czech Republic*
[6]*IRFU, CEA, Université Paris-Saclay, 91191 Gif-sur-Yvette, France*
[7]*Universität Bochum, Institut für Experimentalphysik, 44780 Bochum, Germany*
[8]*Universität Bonn, Helmholtz-Institut für Strahlen- und Kernphysik, 53115 Bonn, Germany*
[9]*Universität Bonn, Physikalisches Institut, 53115 Bonn, Germany*

[*]Corresponding author.
[‖]Present address: NISER, Centre for Medical and Radiation Physics, Bubaneswar, India.
[††]Also at KEK, 1-1 Oho, Tsukuba, Ibaraki 305-0801, Japan.
[†]Deceased.
[¶¶]Also at Department of Physics, National Kaohsiung Normal University, Kaohsiung County 824, Taiwan.
[§]Also at Institut für Theoretische Physik, Universität Tübingen, 72076 Tübingen, Germany.
[‡]Also at ORIGINS Excellence Cluster, 85748 Garching, Germany.
[¶]Also at University of Eastern Piedmont, 15100 Alessandria, Italy.
[**]Also at Chubu University, Kasugai, Aichi 487-8501, Japan.

[10]Universität Freiburg, Physikalisches Institut, 79104 Freiburg, Germany
[11]Universität Mainz, Institut für Kernphysik, 55099 Mainz, Germany
[12]Technische Universität München, Physik Dept., 85748 Garching, Germany
[13]Ludwig-Maximilians-Universität, 80539 München, Germany
[14]Matrivani Institute of Experimental Research & Education, Calcutta-700 030, India
[15]Tel Aviv University, School of Physics and Astronomy, 69978 Tel Aviv, Israel
[16]Abdus Salam ICTP, 34151 Trieste, Italy
[17]Trieste Section of INFN, 34127 Trieste, Italy
[18]University of Trieste, Dept. of Physics, 34127 Trieste, Italy
[19]Torino Section of INFN, 10125 Torino, Italy
[20]University of Torino, Dept. of Physics, 10125 Torino, Italy
[21]University of Miyazaki, Miyazaki 889-2192, Japan
[22]Yamagata University, Yamagata 992-8510, Japan
[23]National Centre for Nuclear Research, 02-093 Warsaw, Poland
[24]Warsaw University of Technology, Institute of Radioelectronics, 00-665 Warsaw, Poland
[25]University of Warsaw, Faculty of Physics, 02-093 Warsaw, Poland
[26]University of Aveiro, I3N, Dept. of Physics, 3810-193 Aveiro, Portugal
[27]LIP, 1649-003 Lisbon, Portugal
[28]Affiliated with an international laboratory covered by a cooperation agreement with CERN
[29]Affiliated with an institute covered by a cooperation agreement with CERN
[30]CERN, 1211 Geneva 23, Switzerland
[31]Academia Sinica, Institute of Physics, Taipei 11529, Taiwan
[32]Center for High Energy and High Field Physics and Dept. of Physics, National Central University, 300 Zhongda Rd., Zhongli 320317, Taiwan
[33]University of Illinois at Urbana-Champaign, Dept. of Physics, Urbana, Illinois 61801-3080, USA

(Received 28 December 2023; revised 27 April 2024; accepted 14 May 2024; published 14 August 2024)

The COMPASS Collaboration performed measurements of the Drell-Yan process in 2015 and 2018 using a 190 GeV/c π^- beam impinging on a transversely polarized ammonia target. Combining the data of both years, we present final results on the amplitudes of five azimuthal modulations, which correspond to transverse-spin-dependent azimuthal asymmetries (TSAs) in the dimuon production cross section. Three of them probe the nucleon leading-twist Sivers, transversity, and pretzelosity transverse-momentum dependent (TMD) parton distribution functions (PDFs). The other two are induced by subleading effects. These TSAs provide unique new inputs for the study of the nucleon TMD PDFs and their universality properties. In particular, the Sivers TSA observed in this measurement is consistent with the fundamental QCD prediction of a sign change of naive time-reversal-odd TMD PDFs when comparing the Drell-Yan process with deep inelastic scattering. Also, within the context of model predictions, the observed transversity TSA is consistent with the expectation of a sign change for the Boer-Mulders function.

DOI: 10.1103/PhysRevLett.133.071902

After decades of extensive theoretical studies and experimental efforts, enormous progress has been made in the study of the internal structure of nucleons. However, a full understanding of the nucleon structure in terms of quarks and gluons remains an open challenge. When exploring the three-dimensional parton structure of hadrons in momentum space, two types of measurements are of particular importance: first, the semi-inclusive measurements of hadron production in deep inelastic lepton-nucleon scattering, $\ell N \to \ell' hX$, hereafter referred to as SIDIS; second, the Drell-Yan process, i.e., quark–antiquark annihilation into a pair of oppositely charged leptons (dileptons) in hadron-nucleon collisions, $hN \to \ell\bar{\ell}X$, hereafter referred to as DY.

The cross section can, in both cases, be factorized into convolutions of perturbatively calculable hard-scattering parton cross sections and nonperturbative functions. The latter are the parton distribution functions (PDFs) describing the distribution of quarks in the target nucleon and either the functions describing the fragmentation of a quark into the observed hadron (in SIDIS) or the quark PDFs of the incoming hadron (in DY) [1–9].

The three-dimensional picture of hadrons involves both the longitudinal and the intrinsic transverse motion of partons inside (un)polarized hadrons, as well as the spin degrees of freedom. Within the leading-twist (twist-2) approximation of pQCD, there exist eight transverse-momentum-dependent (TMD) PDFs of the nucleon describing the distributions of longitudinal and transverse momenta of partons and their correlations with nucleon and quark spins.

These eight TMD PDFs are expected to be universal and process independent for the set of processes, for which standard TMD factorization theorems exist (e.g., SIDIS, DY) [6]. However, within the TMD framework of QCD, the two naively time-reversal-odd TMD PDFs $f_{1T}^{\perp}$ and $h_1^{\perp}$, i.e., the quark Sivers [10] and Boer-Mulders [11] functions, are predicted to have the same magnitudes but opposite signs when comparing DY and SIDIS [12–14]. The experimental test of this fundamental prediction is a major challenge in hadron physics.

The functions $f_{1T}^{\perp}$, $h_1^{\perp}$, and other TMD PDFs are accessed via measurements of specific azimuthal asymmetries in SIDIS and DY (for recent reviews and global fit results see, e.g., Refs. [15–23]). The COMPASS experiment at CERN [24,25] has the unique capability to explore the transverse-spin structure of the nucleon in a kinematic region that is similar for SIDIS and DY. This mitigates the uncertainties of scale dependence (the TMD evolution [6,26–29]) in the comparison of the TMD PDFs extracted from these two measurements, while studying their process (in)dependence.

In 2017, COMPASS reported the results of the first ever DY measurement with a polarized target [30]. A first measurement of the Sivers effect in $W^{\pm}$ and Z^0-boson production in collisions of transversely polarized protons at RHIC was reported by the STAR Collaboration [31,32]. Both measurements showed some evidence for the sign-change property of the Sivers function. New DY data with transversely polarized protons were collected by COMPASS in 2018. In this Letter, we report results from the combined analysis of the COMPASS DY data collected in 2015 and 2018. Both datasets are similar in size.

Following the conventions of Refs. [25,30,33], the general expression for the differential cross section of pion-induced DY lepton-pair production off a transversely polarized nucleon can be written as follows:

$$\begin{aligned}\frac{d\sigma}{dq^4 d\Omega} \propto\ & (F_U^1 + F_U^2)(1 + A_{\mathrm{U}}^1 \cos^2\theta_{\mathrm{CS}}) \\ & \times \Big\{1 + S_T \big[D_1 A_{\mathrm{T}}^{\sin\varphi_{\mathrm{S}}} \sin\varphi_{\mathrm{S}} \\ & + D_2 \big(A_{\mathrm{T}}^{\sin(2\varphi_{\mathrm{CS}}+\varphi_{\mathrm{S}})} \sin(2\varphi_{\mathrm{CS}} + \varphi_{\mathrm{S}}) \\ & \quad + A_{\mathrm{T}}^{\sin(2\varphi_{\mathrm{CS}}-\varphi_{\mathrm{S}})} \sin(2\varphi_{\mathrm{CS}} - \varphi_{\mathrm{S}})\big) \\ & + D_3 \big(A_{\mathrm{T}}^{\sin(\varphi_{\mathrm{CS}}+\varphi_{\mathrm{S}})} \sin(\varphi_{\mathrm{CS}} + \varphi_{\mathrm{S}}) \\ & \quad + A_{\mathrm{T}}^{\sin(\varphi_{\mathrm{CS}}-\varphi_{\mathrm{S}})} \sin(\varphi_{\mathrm{CS}} - \varphi_{\mathrm{S}})\big)\big]\Big\}. \end{aligned} \tag{1}$$

Here, q is the four-momentum of the exchanged virtual photon, F_U^1, F_U^2 are polarization- and azimuth-independent structure functions, and the polar asymmetry A_{U}^1 (often referred to as λ) is given as $A_{\mathrm{U}}^1 = (F_U^1 - F_U^2)/(F_U^1 + F_U^2)$. The subscript $(U)T$ denotes (in)dependence on the transverse polarization of the target. In analogy to SIDIS, the virtual-photon depolarization factors are given as $D_1 = (1+\cos^2\theta_{\mathrm{CS}})/(1+\lambda\cos^2\theta_{\mathrm{CS}})$, $D_2 = \sin^2\theta_{\mathrm{CS}}/(1+\lambda\cos^2\theta_{\mathrm{CS}})$ and $D_3 = \sin 2\theta_{\mathrm{CS}}/(1+\lambda\cos^2\theta_{\mathrm{CS}})$. At leading order of pQCD, within the twist-2 approximation, $F_U^2 = 0$ and $\lambda = 1$. The angle φ_{S} defined in the target rest frame is the relative azimuthal angle between the transverse component of the virtual-photon momentum, q_{T}, and the direction of the nucleon transverse polarization S_{T} (see Ref. [30]). The azimuthal angle φ_{CS} and the polar angle θ_{CS} of the lepton, as well as its solid angle Ω, are defined in the Collins-Soper frame following Refs. [30,33].

In Eq. (1), the transverse-spin-dependent asymmetries A_T^w (hereafter referred to as TSAs) are the amplitudes of the azimuthal modulations $w = w(\varphi_{\mathrm{S}}, \varphi_{\mathrm{CS}})$, divided by the polarization- and azimuth-independent part of the DY cross section and the corresponding depolarization factor. The cross section comprises five TSAs. Three of them can be described by contributions from twist-2 TMD PDFs, while the other two arise due to higher-twist PDFs related to quark-gluon correlations, which induce a suppression by a factor Q^{-1}. The three DY twist-2 TSAs, $A_{\mathrm{T}}^{\sin\varphi_{\mathrm{S}}}$, $A_{\mathrm{T}}^{\sin(2\varphi_{\mathrm{CS}}-\varphi_{\mathrm{S}})}$ and $A_{\mathrm{T}}^{\sin(2\varphi_{\mathrm{CS}}+\varphi_{\mathrm{S}})}$ are related to the nucleon Sivers ($f_{1T}^{\perp}$), transversity (h_1) and pretzelosity ($h_{1T}^{\perp}$) TMD PDFs, respectively [33,34]. In the Sivers TSA, the nucleon TMD PDFs are convoluted with the spin-independent pion TMD PDFs $f_{1,\pi}$, while for the other two TSAs the convolution involves the pion Boer-Mulders TMD PDFs $h_{1,\pi}^{\perp}$. For convenience, these TSAs are hereafter called Sivers TSA, transversity TSA, and pretzelosity TSA.

In the case of unpolarized-hadron production in SIDIS of leptons off transversely polarized nucleons, the three aforementioned nucleon TMD PDFs induce analogous twist-2 TSAs [33–36]. Experimentally, these TSAs were investigated by HERMES using a proton target [37,38], by COMPASS using both proton and deuteron targets [37,39–44] and at JLab using a neutron target [45]. Nonzero quark Sivers and transversity TMD PDFs were extracted from SIDIS measurements, using both collinear [17,18,46–48] and TMD [19–21,26–28,49–53] evolution approaches. Possible relations between collinear and TMD distributions and the matching of corresponding factorization and evolution schemes are the subject of dedicated studies [9,54–56].

The dimuon production data were collected by the COMPASS experiment in 2015 and in 2018 using the 190 GeV/c secondary π^- beam with an average intensity of 0.7×10^8 s^{-1}, delivered from the M2 beam line in the north area of the super proton synchrotron (SPS) complex

at CERN [57]. Beam particles were scattered off a set of consecutive cylindrical targets, mounted coaxially along the beam axis, which is chosen as the z axis of the spectrometer. The polarized proton (NH_3) target consisted of two cylindrical cells, each 55 cm long and 4 cm in diameter [58]. The two cells were polarized vertically (transverse to the beam axis) in opposite directions, allowing data to be taken with up- and down-spin orientations simultaneously. In order to compensate for the differences in the dimuon acceptance of the two cells, the polarization of the target was periodically reversed. The reversals were performed nearly every two weeks to reduce possible acceptance variations over time. The target transverse polarization was preserved using a 0.6 T dipole magnetic field with a relaxation time of about 1000 h [58]. The magnitude of the average proton polarization during the 2015 and 2018 measurements was $\langle P_T \rangle \approx 0.7$. The resolution of the reconstructed interaction vertex position along the z axis was estimated to be of order of 10 cm for the DY events produced in the polarized target region. The cells were separated by a 20 cm gap to minimize migration of events from one cell to the other. The dilution factor, accounting for the fraction of polarizable nucleons in the target and the migration of reconstructed events from one target cell to the other, was calculated to be $\langle f \rangle \approx 0.18$ [59]. Both contributions were evaluated as a function of kinematic variables and were taken into account on an event-by-event basis.

A 240 cm long hadron absorber made of aluminium oxide with a cylindrical tungsten core of 5 cm in diameter was placed 135 cm downstream of the polarized target.

The COMPASS spectrometer configuration used during the DY measurements was essentially the same as during SIDIS measurements [24,39,43]. The hadrons produced in pion-nucleon interactions in the target region were mostly stopped by the absorber. Charged particles were detected by the system of tracking detectors in the two-stage spectrometer. The COMPASS muon identification systems, consisting of a set of large-area trackers and hadron absorbers, allowed the selection of muon tracks. The triggering of dimuon events required the hit pattern of several hodoscope planes to be consistent with two muon candidates originating from the target region. These hodoscope systems covered a wide acceptance in muon polar angle θ_μ (8 mrad $< \theta_\mu <$ 160 mrad).

The physics data taking in 2015 (2018) was performed in nine (eight) periods, each consisting of two consecutive, about week-long subperiods with opposite target polarizations. For the analysis presented in this Letter, both 2015 and 2018 data were iteratively reprocessed, improving detector calibrations and alignment, and optimizing the reconstruction settings.

The data collected in each given (sub-)period were analyzed independently for possible instabilities of kinematic and azimuthal distributions, which could be due to unnoticed detector or trigger problems. Dimuon event candidates are selected requiring reconstructed tracks of an incoming pion and at least two oppositely charged outgoing muons associated with a common production vertex. Production vertices are required to be within the fiducial volumes of the polarized-target cells. A set of selection criteria was applied to ensure the quality of the reconstructed tracks, the reliability of the muon identification and to verify that the topology of the dimuon events is consistent with the registered trigger patterns.

The dimuon transverse momentum q_T is required to be above 0.4 GeV/c to ensure sufficient resolution of the azimuthal angles φ_{CS} and φ_S. In order to reduce background from two-muon events that are not produced via the DY process, the dimuon mass range was chosen as $4.0\ \mathrm{GeV}/c^2 < M_{\mu\mu} < 9.0\ \mathrm{GeV}/c^2$. This range was enlarged compared to our previous publication [30], where stricter requirements on the invariant mass range were applied: $4.3\ \mathrm{GeV}/c^2 < M_{\mu\mu} < 8.5\ \mathrm{GeV}/c^2$. At lower masses, the background contamination consists of contributions from ψ', J/ψ, semimuonic open-charm decays and combinatorial background. Choosing the upper limit at 9.0 GeV/c^2 practically eliminates the contribution of Υ-resonances. Based on Monte-Carlo studies (using the PYTHIA-8 generator and the GEANT-4 based COMPASS setup simulation tool), it was observed that the background contribution depends dominantly on the mass. In the first mass bin ($4.00\ \mathrm{GeV}/c^2 < M_{\mu\mu} < 4.36\ \mathrm{GeV}/c^2$), the estimated background amounts to about 30%, with the largest contribution coming from the ψ' tail. It rapidly drops to 6% in the next mass bin ($4.36\,\mathrm{GeV}/c^2 < M_{\mu\mu} < 5.12\,\mathrm{GeV}/c^2$) [59]. Over all the enlarged mass range the background was estimated to be about 10%, while it was below 5% using the previous selection [30]. Recent COMPASS studies indicate that in the ψ' and J/ψ regions, and between them, the asymmetries are small and compatible with zero within 0.5%–2% statistical precision. This suggests that the background represents only a dilution to the DY TSAs. The appropriate weighting factors were evaluated on an event-by-event basis as a function of $M_{\mu\mu}$ and included in the overall dilution factor, assigning an additional 5% normalization uncertainity to it, accounting for possible small background asymmetries. After all selections, about 102000 dimuon events remained for analysis (50000 in 2015 and 52000 in 2018).

The Bjorken scaling variables related to the beam pion, x_π, and the target nucleon, x_N, have the following average values: $\langle x_N \rangle = 0.16$, $\langle x_\pi \rangle = 0.48$. Hence, the kinematic domain explored by the COMPASS measurement probes mainly the valence quark region, where the expected dominant TMD PDF contributions come from the u quarks of the nucleon and the $\bar{u}$ quark of the incoming π^-. The average values for dimuon transverse momentum ($\langle q_T \rangle = 1.2\ \mathrm{GeV}/c$) and invariant mass ($\langle M_{\mu\mu} \rangle = 5.1\ \mathrm{GeV}/c^2$)

satisfy the requirements imposed by the factorization theorems [52].

For each data-taking year separately, all five TSAs present in the cross section [see Eq. (1)] are extracted period by period and then averaged. The extraction of the asymmetries is performed using an extended unbinned maximum likelihood estimator, where all five modulations are fitted simultaneously using dimuon events produced in each target cell for the two directions of the target polarization. The estimator is based on the method developed for the COMPASS SIDIS TSA analyses [65]. In this approach, flux and acceptance-dependent systematic uncertainties are minimized. The TSAs are evaluated in one-dimensional kinematic bins as a function of x_N, x_π, dimuon Feynman variable x_F, q_T, or $M_{\mu\mu}$, integrating over the entire accepted range of all other variables. In order to evaluate the TSAs, the amplitudes of the modulations are corrected for the depolarization factors and for the effective proton polarization $f \cdot \langle P_T \rangle$. The depolarization factors and the dilution factor are applied as weights on an event-by-event basis. The depolarization factors are evaluated using the approximation $\lambda = 1$. Known deviations from this assumption with λ ranging between 0.5 and 1 [66–68] decrease the normalization by at most 5%. This effect is not included in the total uncertainties. The largest systematic uncertainties for the TSAs are attributed to residual variations of the experimental conditions. Such instabilities may result in changes of the spectrometer acceptance, which may not be entirely cancelled when combining the data in a given period. The corresponding systematic effects are quantified by evaluating various types of false asymmetries, similar to the COMPASS SIDIS analyses [40,69], and by checking the stability of the results over the periods. Thorough studies performed separately for the two data-taking years revealed somewhat larger systematic effects and instabilities for 2018 compared to 2015. The systematic point-to-point uncertainties associated with the TSAs were estimated to be between 0.7 to 0.8 times the corresponding statistical uncertainties in 2015 and between 1.0 to 1.2 in 2018. For the two years, the normalization uncertainties associated with target polarization and overall dilution factor are 5% and 12%, respectively. For each TSA, the 2015 and 2018 results are combined by calculating the weighted average in each kinematic bin, taking into account the quadratically added statistical and systematic uncertainties.

In Fig. 1, the combined 2015 and 2018 COMPASS results obtained for the three twist-2 TSAs $A_T^{\sin\varphi_S}$, $A_T^{\sin(2\varphi_{CS}+\varphi_S)}$, and $A_T^{\sin(2\varphi_{CS}-\varphi_S)}$ are shown as a function of the variables x_N, x_π, x_F, q_T, and $M_{\mu\mu}$. Compared to the previous analysis of only the 2015 data [30], adding the 2018 data and enlarging the dimuon mass range increased the statistical precision of the measurement by a factor of 1.5 [59]. The presented TSAs are compared with recent theoretical predictions, which are based on calculations performed in Ref. [52]. These predictions are obtained by

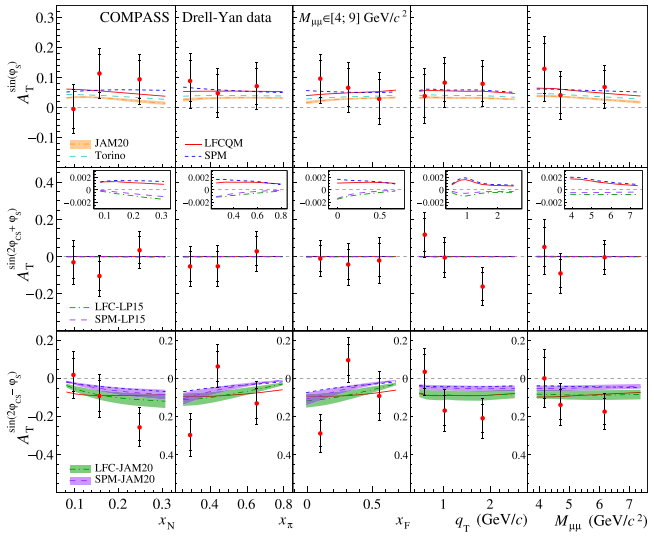

FIG. 1. Kinematic dependences of the Sivers, pretzelosity, and transversity TSAs (top to bottom). Inner (outer) error bars represent statistical (total experimental) uncertainties. For theoretical predictions see text.

using for each bin the appropriate average kinematic values given by the event population. For each TSA, four different calculations based on two different approaches are presented. The first approach is solely based on model predictions for pion and proton TMD PDFs using the light-front constituent quark model (LFCQM) [70–77] and the spectator model (SPM) [78–82]. The second is a "hybrid" approach, in which model inputs are restricted to the usage of LFCQM and SPM for the pion Boer-Mulders function, while the nonperturbative inputs for the proton TMD PDFs are taken from available parametrizations extracted from experimental data ("Torino" fit [48], "JAM20" global fit [53] and "LP15" fit [83]). The MSTW extraction [84] was used for the collinear proton PDF $f_{1,p}$, while for the collinear pion PDF $f_{1,\pi}$ the SMRS [85] fits were used. In these predictions, the TMD evolution is implemented at next-to-leading logarithmic precision for all twist-2 TSAs. The model calculations were performed using the sign-change hypothesis for both the nucleon Sivers and Boer-Mulders TMD PDFs [52,86]. Within the current experimental precision, the models considered here are consistent with the data, and none can be considered preferred.

The Sivers TSA $A_T^{\sin\varphi_S}$ is predicted to be positive in the entire kinematic range [52], which is in agreement with the COMPASS data points shown in Fig. 1. The average Sivers TSA, $\langle A_T^{\sin\varphi_S} \rangle = 0.070 \pm 0.037(\text{stat}) \pm 0.031(\text{syst})$, is found to be above zero at about 1.5 standard deviations of the total uncertainty. In the left panel of Fig. 2, the Sivers TSA is shown together with model predictions [52] evaluated with and without the sign-change hypothesis, shown as dark-shaded curves in the top and light-shaded

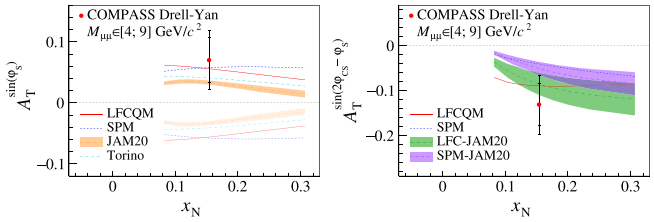

FIG. 2. Left panel: Measured average Sivers TSA and theoretical predictions from different models from Ref. [52]. The dark-shaded (light-shaded) predictions are evaluated with (without) the sign-change hypothesis. Right panel: Measured average transversity TSA and theoretical predictions from different models from Ref. [52]. Otherwise as in Fig. 1.

curves in the bottom of the figure, respectively. Using the band of the presented model predictions, the COMPASS measurement is found to agree with the sign-change hypothesis within less than 1 standard deviation of its total uncertainty, while being away from the no-sign-change hypothesis by about 2.5 to 3 standard deviations. In addition, the present results do not support earlier expectations of a large Sivers effect in the DY process at COMPASS kinematics [25].

The transversity TSA $A_T^{\sin(2\varphi_{CS}-\varphi_S)}$ is expected to be negative, but larger in absolute value compared to the Sivers TSA [52,87]. The average value for the transversity TSA is measured to be below zero with a significance of about 2 standard deviations, $\langle A_T^{\sin(2\varphi_{CS}-\varphi_S)}\rangle = -0.131 \pm 0.046(\text{stat}) \pm 0.047(\text{syst})$. In the right panel of Fig. 2, the average transversity TSA is shown together with model calculations [52]. The COMPASS measurement is found to agree in sign and magnitude with the band of available model predictions, which supports the universal nature of the transversity TMD PDFs.

As discussed in Refs. [52,86], the negative sign of the transversity TSA implies a positive sign of the $\bar{u}\,\pi^-$ Boer-Mulders TMD PDF. Together with the positive sign of the $\cos(2\varphi_{CS})$ modulation found in the unpolarized Drell-Yan data taken with a π^- beam [66,67], which suggests the same sign for the $\bar{u}$ pion and u proton Boer-Mulders TMD PDFs, it follows that the latter function has a positive sign in the Drell-Yan process. Since this positive sign is opposite to the negative sign found for this function in SIDIS [88,89], the present TSA data strongly support the sign change of the proton Boer-Mulders function between DY and SIDIS. We note that all theory calculations shown in Figs. 1 and 2 for the transversity TSA assume such a sign change for the proton Boer-Mulders TMD PDF.

The pretzelosity TSA $A_T^{\sin(2\varphi_{CS}+\varphi_S)}$ is predicted to be very small, which is explained by the magnitude of the pretzelosity TMD PDFs and kinematic suppression factors [52]. The measured average value, $\langle A_T^{\sin(2\varphi_{CS}+\varphi_S)}\rangle = -0.027 \pm 0.046(\text{stat}) \pm 0.043(\text{syst})$, is indeed found to be small and compatible with zero within uncertainties. For the two higher-twist TSAs, the averaged values $\langle A_T^{\sin(\varphi_{CS}-\varphi_S)}\rangle = 0.113 \pm 0.076(\text{stat}) \pm 0.071(\text{syst})$ and $\langle A_T^{\sin(\varphi_{CS}+\varphi_S)}\rangle = -0.071 \pm 0.071(\text{stat}) \pm 0.064(\text{syst})$ are consistent with zero within about 1 standard deviation of the total uncertainty. Compared to the twist-2 TSAs, the statistical uncertainties of the two TSAs related to higher-twist TMD PDFs are notably larger, which is explained by the relative smallness of the depolarization factor D_3. No predictions are available for these twist-3 TSAs. The full set of numerical values for the extended and the narrower mass ranges is available upon request.

The new COMPASS results presented in this Letter supersede the previous ones from our first publication [30]. They demonstrate the importance and the potential of measuring the DY process with transversely polarized nucleon targets, thereby paving the way for new projects aiming to perform similar studies at CERN and elsewhere [90–92].

Acknowledgments—We gratefully acknowledge the support of the CERN management and staff and the skill and effort of the technicians of our collaborating institutes. We are grateful to S. Bastami and the authors of Ref. [52] for providing us with numerical values of their model predictions. This work was made possible by the financial support of our funding agencies: the Higher Education and Science Committee of the Republic of Armenia, in the frame of the research project No. 21AG-1C028 (Armenia); the MEYS Grants No. LM2023040, No. LM2018104 and No. LTT17018 (Czech Republic); the Charles University Grant No. PRIMUS/22/SCI/017 (Czech Republic); the BMBF Bundesministerium für Bildung und Forschung (Germany); the DFG cluster of excellence "Origin and Structure of the Universe" (Germany); the B. Sen fund (India); the Israel Academy of Sciences and Humanities; the Funds for Research 2019-22 of the University of Eastern Piedmont (Italy); the MEXT and JSPS under Grants No. 18002006, No. 20540299, No. 18540281 and No. 26247032 (Japan); the Daiko and Yamada Foundations (Japan); the NCN (Poland) Grant No. 2020/37/B/ST2/01547; the FCT Grants DOI 10.54499/CERN/FIS-PAR/0022/2019 and DOI 10.54499/CERN/FIS-PAR/0016/2021 (Portugal); the Ministry of Science and Technology (Taiwan); the National Science Foundation, Grant No. PHY-1506416 (USA); the European Union's Horizon 2020 research and innovation programme under Grant Agreement STRONG–2020—No. 824093.

[1] J. C. Collins, D. E. Soper, and G. F. Sterman, Nucl. Phys. **B250**, 199 (1985).
[2] J. C. Collins and D. E. Soper, Nucl. Phys. **B193**, 381 (1981); **B213**, 545(E) (1983).
[3] X. Ji, J. P. Ma, and F. Yuan, Phys. Rev. D **71**, 034005 (2005).
[4] X. Ji, J.-W. Qiu, W. Vogelsang, and F. Yuan, Phys. Lett. B **638**, 178 (2006).

[5] X. Ji, J. W. Qiu, W. Vogelsang, and F. Yuan, Phys. Rev. D **73**, 094017 (2006).
[6] J. Collins, *Foundations of Perturbative QCD* (Cambridge University Press, Cambridge, England, 2013).
[7] S. M. Aybat and T. C. Rogers, Phys. Rev. D **83**, 114042 (2011).
[8] J. P. Ma and G. P. Zhang, J. High Energy Phys. 02 (2014) 100.
[9] J. Collins, L. Gamberg, A. Prokudin, T. C. Rogers, N. Sato, and B. Wang, Phys. Rev. D **94**, 034014 (2016).
[10] D. W. Sivers, Phys. Rev. D **41**, 83 (1990).
[11] D. Boer and P. J. Mulders, Phys. Rev. D **57**, 5780 (1998).
[12] J. C. Collins, Phys. Lett. B **536**, 43 (2002).
[13] S. J. Brodsky, D. S. Hwang, and I. Schmidt, Phys. Lett. B **530**, 99 (2002).
[14] S. J. Brodsky, D. S. Hwang, and I. Schmidt, Nucl. Phys. **B642**, 344 (2002).
[15] M. Anselmino, A. Mukherjee, and A. Vossen, Prog. Part. Nucl. Phys. **114**, 103806 (2020).
[16] H. Avakian, B. Parsamyan, and A. Prokudin, Riv. Nuovo Cimento **42**, 1 (2019).
[17] M. Radici and A. Bacchetta, Phys. Rev. Lett. **120**, 192001 (2018).
[18] J. Benel, A. Courtoy, and R. Ferro-Hernandez, Eur. Phys. J. C **80**, 465 (2020).
[19] A. Bacchetta, F. Delcarro, C. Pisano, and M. Radici, Phys. Lett. B **827**, 136961 (2022).
[20] L. Gamberg, M. Malda, J. A. Miller, D. Pitonyak, A. Prokudin, and N. Sato (Jefferson Lab Angular Momentum (JAM) Collaboration), Phys. Rev. D **106**, 034014 (2022).
[21] M. Bury, A. Prokudin, and A. Vladimirov, J. High Energy Phys. 05 (2021) 151.
[22] S. Bhattacharya, Z.-B. Kang, A. Metz, G. Penn, and D. Pitonyak, Phys. Rev. D **105**, 034007 (2022).
[23] U. D'Alesio, C. Flore, and A. Prokudin, Phys. Lett. B **803**, 135347 (2020).
[24] P. Abbon *et al.* (COMPASS Collaboration), Nucl. Instrum. Methods Phys. Res., Sect. A **577**, 455 (2007).
[25] F. Gautheron *et al.* (COMPASS Collaboration), Report No. SPSC-P-340, CERN-SPSC-2010-014.
[26] S. M. Aybat, A. Prokudin, and T. C. Rogers, Phys. Rev. Lett. **108**, 242003 (2012).
[27] M. Anselmino, M. Boglione, and S. Melis, Phys. Rev. D **86**, 014028 (2012).
[28] M. G. Echevarria, A. Idilbi, Z.-B. Kang, and I. Vitev, Phys. Rev. D **89**, 074013 (2014).
[29] I. Scimemi and A. Vladimirov, J. High Energy Phys. 06 (2020) 137.
[30] M. Aghasyan *et al.* (COMPASS Collaboration), Phys. Rev. Lett. **119**, 112002 (2017).
[31] L. Adamczyk *et al.* (STAR Collaboration), Phys. Rev. Lett. **116**, 132301 (2016).
[32] STAR Collaboration, arXiv:2308.15496.
[33] S. Arnold, A. Metz, and M. Schlegel, Phys. Rev. D **79**, 034005 (2009).
[34] A. Bacchetta, M. Diehl, K. Goeke, A. Metz, P. J. Mulders, and M. Schlegel, J. High Energy Phys. 02 (2007) 093.
[35] P. J. Mulders and R. D. Tangerman, Nucl. Phys. **B461**, 197 (1996); **B484**, 538(E) (1997).
[36] A. Kotzinian, Nucl. Phys. **B441**, 234 (1995).
[37] A. Airapetian *et al.* (HERMES Collaboration), Phys. Rev. Lett. **103**, 152002 (2009).
[38] A. Airapetian *et al.* (HERMES Collaboration), J. High Energy Phys. 12 (2020) 010.
[39] M. Alekseev *et al.* (COMPASS Collaboration), Phys. Lett. B **673**, 127 (2009).
[40] C. Adolph *et al.* (COMPASS Collaboration), Phys. Lett. B **717**, 383 (2012).
[41] C. Adolph *et al.* (COMPASS Collaboration), Phys. Lett. B **736**, 124 (2014).
[42] C. Adolph *et al.* (COMPASS Collaboration), Phys. Lett. B **744**, 250 (2015).
[43] C. Adolph *et al.* (COMPASS Collaboration), Phys. Lett. B **770**, 138 (2017).
[44] B. Parsamyan (COMPASS Collaboration), Phys. Part. Nucl. **45**, 158 (2014).
[45] X. Qian *et al.* (Jefferson Lab Hall A Collaboration), Phys. Rev. Lett. **107**, 072003 (2011).
[46] M. Anselmino, M. Boglione, U. D'Alesio, A. Kotzinian, F. Murgia, and A. Prokudin, Phys. Rev. D **72**, 094007 (2005).
[47] M. Anselmino, M. Boglione, U. D'Alesio, A. Kotzinian, S. Melis, F. Murgia, A. Prokudin, and C. Turk, Eur. Phys. J. A **39**, 89 (2009).
[48] M. Anselmino, M. Boglione, U. D'Alesio, S. Melis, F. Murgia, and A. Prokudin, Phys. Rev. D **87**, 094019 (2013).
[49] M. Anselmino, M. Boglione, U. D'Alesio, F. Murgia, and A. Prokudin, J. High Energy Phys. 04 (2017) 046.
[50] P. Sun and F. Yuan, Phys. Rev. D **88**, 114012 (2013).
[51] S. Bastami *et al.*, J. High Energy Phys. 06 (2019) 007.
[52] S. Bastami, L. Gamberg, B. Parsamyan, B. Pasquini, A. Prokudin, and P. Schweitzer, J. High Energy Phys. 02 (2021) 166.
[53] J. Cammarota, L. Gamberg, Z.-B. Kang, J. A. Miller, D. Pitonyak, A. Prokudin, T. C. Rogers, and N. Sato (Jefferson Lab Angular Momentum Collaboration), Phys. Rev. D **102**, 054002 (2020).
[54] M. G. Echevarria, T. Kasemets, J.-P. Lansberg, C. Pisano, and A. Signori, Phys. Lett. B **781**, 161 (2018).
[55] I. Scimemi, A. Tarasov, and A. Vladimirov, J. High Energy Phys. 05 (2019) 125.
[56] O. del Rio, A. Prokudin, I. Scimemi, and A. Vladimirov, arXiv:2402.01836.
[57] N. Doble, L. Gatignon, K. Hübner, and E. Wilson, Adv. Ser. Dir. High Energy Phys. **27**, 135 (2017).
[58] V. Andrieux *et al.*, Nucl. Instrum. Methods Phys. Res., Sect. A **1025**, 166069 (2022).
[59] See Supplemental Material at http://link.aps.org/supplemental/10.1103/PhysRevLett.133.071902, which includes Refs. [60–64], detailed discussion on the dilution factor calculation and background fractions, a comparison with our first publication [30], and a set of supporting figures.
[60] J. M. Campbell and R. K. Ellis, Phys. Rev. D **60**, 113006 (1999).
[61] J. M. Campbell, R. K. Ellis, and W. T. Giele, Eur. Phys. J. C **75**, 246 (2015).
[62] R. Boughezal, J. M. Campbell, R. K. Ellis, C. Focke, W. Giele, X. Liu, F. Petriello, and C. Williams, Eur. Phys. J. C **77**, 7 (2017).
[63] K. Kovarik *et al.*, Phys. Rev. D **93**, 085037 (2016).
[64] M. Gluck, E. Reya, and A. Vogt, Z. Phys. C **53**, 651 (1992).

[65] C. Adolph *et al.* (COMPASS Collaboration), Phys. Lett. B **713**, 10 (2012).
[66] M. Guanziroli *et al.* (NA10 Collaboration), Z. Phys. C **37**, 545 (1988).
[67] J. S. Conway *et al.* (E615 Collaboration), Phys. Rev. D **39**, 92 (1989).
[68] M. Lambertsen and W. Vogelsang, Phys. Rev. D **93**, 114013 (2016).
[69] C. Adolph *et al.* (COMPASS Collaboration), Phys. Lett. B **717**, 376 (2012).
[70] C. Lorcé, B. Pasquini, and P. Schweitzer, Eur. Phys. J. C **76**, 415 (2016).
[71] B. Pasquini, S. Cazzaniga, and S. Boffi, Phys. Rev. D **78**, 034025 (2008).
[72] B. Pasquini and F. Yuan, Phys. Rev. D **81**, 114013 (2010).
[73] C. Lorcé, B. Pasquini, and M. Vanderhaeghen, J. High Energy Phys. 05 (2011) 041.
[74] S. Boffi, A. V. Efremov, B. Pasquini, and P. Schweitzer, Phys. Rev. D **79**, 094012 (2009).
[75] B. Pasquini and P. Schweitzer, Phys. Rev. D **83**, 114044 (2011).
[76] B. Pasquini and P. Schweitzer, Phys. Rev. D **90**, 014050 (2014).
[77] C. Lorcé, B. Pasquini, and M. Vanderhaeghen, J. High Energy Phys. 01 (2015) 103.
[78] R. Jakob, P. J. Mulders, and J. Rodrigues, Nucl. Phys. **A626**, 937 (1997).
[79] Z. Lu and B.-Q. Ma, Phys. Rev. D **70**, 094044 (2004).
[80] L. P. Gamberg, G. R. Goldstein, and M. Schlegel, Phys. Rev. D **77**, 094016 (2008).
[81] A. Bacchetta, F. Conti, and M. Radici, Phys. Rev. D **78**, 074010 (2008).
[82] L. Gamberg and M. Schlegel, Phys. Lett. B **685**, 95 (2010).
[83] C. Lefky and A. Prokudin, Phys. Rev. D **91**, 034010 (2015).
[84] M. Anselmino, M. Boglione, J. O. Gonzalez Hernandez, S. Melis, and A. Prokudin, J. High Energy Phys. 04 (2014) 005.
[85] P. J. Sutton, A. D. Martin, R. G. Roberts, and W. J. Stirling, Phys. Rev. D **45**, 2349 (1992).
[86] J.-C. Peng, EPJ Web Conf. **85**, 01009 (2015).
[87] A. N. Sissakian, O. Yu. Shevchenko, A. P. Nagaitsev, and O. N. Ivanov, Phys. Part. Nucl. **41**, 64 (2010).
[88] V. Barone, S. Melis, and A. Prokudin, Phys. Rev. D **81**, 114026 (2010).
[89] V. Barone, S. Melis, and A. Prokudin, Phys. Rev. D **82**, 114025 (2010).
[90] C. A. Aidala *et al.* (The LHCSpin Project Collaboration), arXiv:1901.08002.
[91] C. Barschel *et al.*, *LHC Fixed Target Experiments: Report from the LHC Fixed Target Working Group of the CERN Physics Beyond Colliders Forum*, CERN Yellow Reports: Monographs Vol. 4/2020 (CERN, Geneva, 2020).
[92] D. Keller (SpinQuest Collaboration), arXiv:2205.01249.